Carbon 160 (2020) 228–235

Contents lists available at ScienceDirect

Carbon

journal homepage: www.elsevier.com/locate/carbon

Carbon at the nanoscale: Ultrastiffness and unambiguous definition of incompressibility

Almaz Khabibrakhmanov [a, b, c], Pavel Sorokin [a, b, c, *]

[a] Technological Institute for Superhard and Novel Carbon Materials, 108840, 7a Tsentralnaya Street, Troitsk, Moscow, Russian Federation
[b] National University of Science and Technology MISiS, 119049, 4 Leninskiy Prospekt, Moscow, Russian Federation
[c] Moscow Institute of Physics and Technology (National Research University), 141701, 9 Institutskiy lane, Dolgoprudny, Moscow Region, Russian Federation

ARTICLE INFO

Article history:
Received 1 November 2019
Received in revised form
7 December 2019
Accepted 27 December 2019
Available online 2 January 2020

ABSTRACT

In the presented work, the features of mechanical stiffness of carbon nanoparticles (nanodiamonds and fullerenes) in a wide range of sizes are considered. The enhancement of nanodiamonds stiffness (comparing to bulk diamond) is studied and explained in the terms of average bond stiffness k_0. It is shown that k_0 can be useful in the description of various carbon nanostructures and gives reliable estimates of their incompressibility. Moreover, we found that k_0 can be well estimated based only on relaxed atomic geometry.

1. Introduction

Diamond crystal is well-known for the variety of its extraordinary properties. In particular, diamond is famous for the unique mechanical stiffness having the highest bulk modulus and being referred to as the hardest crystalline material [1]. Search for superhard materials still draws close attention of materials scientists and attempts to find materials superior to diamond by stiffness, already counting successful studies of carbon nanotubes [2–4], ultrahard fullerites [5–7] and graphene [8,9], continue to this day.

Nanodiamonds (ND) represent small (several nm in size) diamond particles. From general considerations, it can be supposed that size effects in such particles should lead to modification of the original diamond properties. Structural, electronic and magnetic properties of nanodiamonds attract significant interest and have been studying for decades [10,11]. Special attention was also given to nanocrystalline diamond [12,13] due to its exceptional mechanical stiffness by which it can even exceed single crystal diamond. Nevertheless, the mechanical properties of single nanodiamonds – structural units of nanocrystalline diamond – mainly remained unexplored until recently. However, the latest experimental evidence of nanodiamonds ultrastiffness [14,15] indicates that their mechanical properties also deserve detailed study.

Conventionally, mechanical stiffness is characterized by bulk modulus B_0 as a measure of incompressibility. However, the calculation of elastic moduli for nanostructures can be puzzling due to the ambiguity of volume on the nanoscale. This problem was widely discussed for carbon nanotubes (CNTs) and fullerenes, and many different ways to determine their volume were proposed. Most often CNTs were described as hollow structures with a certain shell thickness t. The *ad hoc* convention is to set $t = 3.4$ Å [16,17] as a value of interlayer spacing in graphite. The alternative approach proposed by Yakobson et al. [18] is based on continuum shell elasticity theory and gives the value of $t = 0.66$ Å. Later, many other approaches for finding shell thickness t were examined [16,17,19]. As for fullerenes, Ruoff et al. were the first to estimate B_0 of C_{60} molecule as 843 GPa [20] and 826 GPa [21]. In both cases, C_{60} was considered as a homogenous elastic solid. With the same assumption, Peón-Escalante et al. [22] theoretically predicted $B_0 = 874$ GPa, but a spherical shell model of C_{60} (with $t = 3.4$ Å) also considered in work [22] led to a significantly lower $B_0 = 640$ GPa.

Thus, there is an explicit problem with calculations of volume and, as a result, with the determination of elastic moduli for nanostructures, and alternative ways to characterize nanostructures mechanical properties should be considered. Here we suggest using average bond stiffness k_0 as a mechanical characteristic of uniform hydrostatic compression. Actually, bond stiffness constants were often used before in studies of nanostructures mechanical properties, mainly to recalculate them into elastic moduli [21,23] with different assumptions about volume, as mentioned above. On the

* Corresponding author. Technological Institute for Superhard and Novel Carbon Materials, 108840, 7a Tsentralnaya street, Troitsk, Moscow, Russian Federation.
E-mail address: PBSorokin@tisnum.ru (P. Sorokin).

https://doi.org/10.1016/j.carbon.2019.12.071
0008-6223/

contrary, we propose to use k_0 as a primary mechanical characteristic of isotropic compression on the nanoscale.

This paper is outlined as follows. In Sec.2, we define average bond stiffness and give details of *ab initio* calculations. The obtained results and discussions are presented in Sec.3. We introduce considered structures of nanodiamonds and fullerenes and briefly report their structural properties. Further, we discuss in details the features of nanodiamonds and fullerenes mechanical stiffness. We present the results for bulk modulus and average bond stiffness and compare these two approaches. We reveal the enhancement of both B_0 and k_0 with decreasing size, but values of B_0 are shown to be dependent on the assumptions made about nanostructures volume. In contrast, we find that k_0 is an unambiguous quantity that enables us to correctly compare various carbon nanostructures with each other as well as with crystalline materials by their mechanical rigidity. We also demonstrate that k_0 could be reasonably estimated based only on relaxed atomic geometry.

2. Methods

2.1. Average bond stiffness

We define average bond stiffness in the following way:

$$k = \frac{1}{N_b}\left(\frac{\partial^2 E}{\partial l^2}\right). \quad (1)$$

here E is total energy, N_b and l are the number of chemical bonds in a structure and their average length, respectively. This physical quantity has units of N m^{-1} and does not require any ill-defined quantities, such as a thickness of atomic monolayer or nanocluster volume, to calculate its value.

As mechanical properties of a covalently bonded solid are completely determined by the properties of its chemical bonds, values of bulk modulus B and average bond stiffness k are not independent and related via the following equation (see the derivation in Supplementary Materials):

$$k = \frac{V_0}{N_b l_0^2}\left[\frac{B}{1+\delta}\left(\frac{\partial\delta}{\partial\varepsilon}\right)^2 - P\left(\frac{\partial^2\delta}{\partial\varepsilon^2}\right)\right], \quad (2)$$

where $\varepsilon = \frac{l-l_0}{l_0}$, $\delta = \frac{V-V_0}{V_0}$ are a linear and volumetric strain, respectively. At zero pressure, it reduces to Eq. (3) that allows estimating bulk modulus based on average bond stiffness:

$$B_0^{est} = k_0 \cdot \frac{N_b l_0^2}{V_0\left(\frac{\partial\delta}{\partial\varepsilon}\right)^2_{\varepsilon=0}}. \quad (3)$$

For two-dimensional materials one can introduce 2D equibiaxial strain (α) and 2D analogs of pressure (F) and bulk modulus (γ, also referred to as layer modulus [24]): $\alpha = \frac{A-A_0}{A_0}$, $F = -\left(\frac{\partial E}{\partial A}\right)$, $\gamma = -A\left(\frac{\partial F}{\partial A}\right) = A\left(\frac{\partial^2 E}{\partial A^2}\right)$, where A is a surface area. Average bond stiffness can be defined in the same way (1), as for bulk solids, and the relation between k and γ is governed by the formula analogous to Eq. (2):

$$k = \frac{A_0}{N_b l_0^2}\left[\frac{\gamma}{1+\alpha}\left(\frac{\partial\alpha}{\partial\varepsilon}\right)^2 - F\left(\frac{\partial^2\alpha}{\partial\varepsilon^2}\right)\right]. \quad (4)$$

2.2. Computational details

All calculations of the atomic structures in this work were done in the framework of density functional theory (DFT) [25,26] using the projector augmented wave (PAW) method [27,28], as implemented in VASP [29,30]. Electron exchange-correlation was treated in generalized gradient approximation as proposed by Perdew-Burke-Ernzerhof [31]. The plane waves energy cutoff was equal to 520 eV in all cases. Nanodiamonds and fullerenes were simulated as isolated nanoparticles surrounded by not less than 1 nm thick vacuum to avoid spurious interactions between periodic images of the structures. Calculations were done only at Γ-point of the corresponding Brillouin zone. Atomic coordinates relaxation was performed until interatomic forces converged to within 0.01 eV Å^{-1}. In the case of bulk diamond and graphene, the **k**-point sampling of Brillouin zone was done using $24 \times 24 \times 24$ and $16 \times 16 \times 1$ Monkhorst-Pack [32] meshes centered at Γ-point, respectively. For graphene, a vacuum space along Z-axis was set as large as 10 Å for the same purpose as in the case of nanoparticles.

3. Results and discussions

3.1. Reference systems

Bulk diamond and graphene were selected as references for mechanical properties calculations in this study due to a pure sp^3- and sp^2-hybridization realized in these materials, respectively. Therefore, the broad spectrum of the mechanical properties possible in covalently bonded carbon systems could be covered.

We scrutinized the mechanical properties of diamond and graphene in a vast range of C–C bond lengths (1.3 – 1.8 Å). The obtained data were fitted to the corresponding 4th order equations of state (EOS) for bulk [36] and two-dimensional [24] materials, respectively. Extracted fitting parameters are given in Table 1. For diamond crystal, bulk modulus and pressure were found as derivatives of the energy with respect to the volume that allows to plot $B(P)$ dependence (Fig. 1a). We compared our data with the previous theoretical [37,38] and experimental findings [33] and discovered a good agreement that verifies the obtained results. Then, the dependences of bond stiffness constant on bond length calculated using Eqs. (2) and (4) were plotted (Fig. 1b).

Although γ_0 and k_0 are quantities very convenient for theoretical considerations, these cannot be directly measured that does not allow for direct comparison with experiment. Elastic moduli (in units of GPa) are usually found instead. Therefore, we reviewed various theoretical as well as experimental works on elastic moduli of diamond and graphene (graphite) and recalculated elastic constants to γ_0 and k_0 (see Table 1). For graphene, only C_{11} and C_{12} are required to estimate γ_0 [24] via $\gamma_0 = \frac{1}{2}(C_{11} + C_{12}) \cdot t$. Here t is a thickness of graphene sheet which was set equal to the interlayer spacing of graphite given in the corresponding work. Then, k_0 was found using Eq. (4) at zero strain: $k_0 = \frac{4A_0\gamma_0}{N_b l_0^2} = 2\sqrt{3}\gamma_0$. For diamond, k_0 was directly estimated from bulk modulus via Eq. (3): $k_0 = \frac{9V_0B_0}{N_b l_0^2} = 3B_0a_0$. The data in Table 1 clearly indicate that our results are well-consistent with previous theoretical and experimental ones.

3.2. Considered structures

We investigated the mechanical properties of nanodiamonds and fullerenes in the wide range of sizes (54–1798 atoms). The set of studied nanodiamonds included 20 structures of cuboctahedral and cubic shapes. All structures were initially cleaved from the bulk diamond lattice, so their surfaces are composed of various low index diamond crystallographic planes. Considered geometrical

Table 1
Theoretical and experimental data on structural and mechanical characteristics of bulk diamond and graphene. Values obtained in the present work are given without superscript symbols. (Layer modulus γ_0 in N m^{-1} and bulk modulus B_0 in GPa, their first derivatives γ_0' and B_0' dimensionless, their second derivatives γ_0'' and B_0'' in m N^{-1} and GPa^{-1}, respectively).

	Graphene		Diamond	
	theory	experiment	theory	experiment
Lattice constant a_0 [Å]	2.468, 2.47[a], 2.446[b]	2.459[c], 2.463[d], 2.462[e]	3.572, 3.572[f], 3.574[g]	3.567[h], 3.566[i], 3.575[j]
Layer modulus γ_0 of graphene and bulk modulus B_0 of diamond and their derivatives	$\gamma_0 = 207.6$ $\gamma_0' = 4.38$ $\gamma_0'' = -0.0398$ $\gamma_0 = 206.6$[a]	$\gamma_0 = 209.4$[d], 209.6[k], 207.7[l]	$B_0 = 434.6$ $B_0' = 3.84$ $B_0'' = -0.0116$ $B_0 = 433$[f]	$B_0 = 442$[m], 442[n], 444.5[i], 438[j]
Bond stiffness constant k_0 [N m^{-1}]	719.1, 715.7[a], 724.9[b]	725.4[d], 726.1[k], 719.5[l]	465.7, 464.0[f], 462.1[g]	473[m], 475.5[i], 469.8[j]

[a] Ref. [24].
[b] Ref. [39].
[c] Ref. [40].
[d] Ref. [41].
[e] Ref. [42].
[f] Ref. [43].
[g] Ref. [44].
[h] Ref. [45].
[i] Ref. [46].
[j] Ref. [33,34].
[k] Ref. [47].
[l] Ref. [48].
[m] Ref. [49].
[n] Ref. [50].

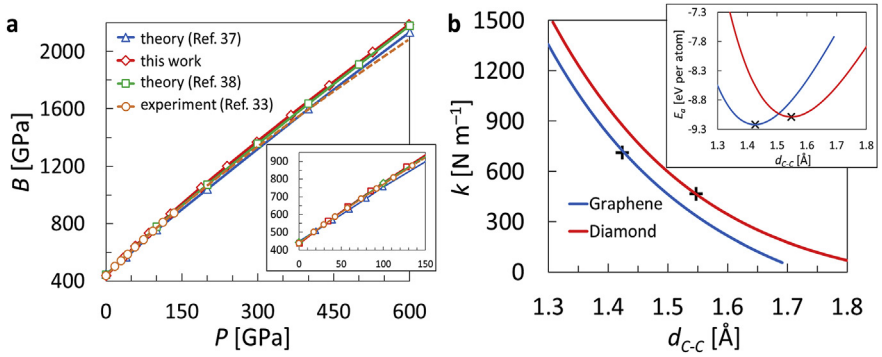

Fig. 1. (a) The dependence of diamond bulk modulus on external pressure. The inset shows the low-pressure region in more details. Circles (up to 140 GPa) indicate experimental data [33], corrected for modifications to pressure calibration [34]. The dashed curve is an extrapolation of these data beyond 140 GPa based on the corresponding Vinet fit [34,35]. (b) The dependence of bond stiffness constant on bond length for graphene and bulk diamond. On the inset, energy per atom vs. bond length curves are drawn. Crosses denote the equilibrium state for each system. (A colour version of this figure can be viewed online.)

shapes and the examples of nanodiamonds atomic structures are depicted in Fig. 2. The cuboctahedral subset of studied nanodiamonds was represented by 5 structures (C_{142}, C_{323}, C_{660}, C_{897}, C_{1201}) faceted with 36% {111} surfaces and 64% {100} surfaces. The first cubic subset – cube {110} – contained 6 structures (C_{54}, C_{259}, C_{509}, C_{712}, C_{1174}, C_{1798}) encased with 67% {110} surfaces and 33% {100} surfaces, and the second one – cube {100} – involved 9 cubic nanodiamonds (C_{75}, C_{239}, C_{387}, C_{568}, C_{577}, C_{812}, C_{920}, C_{1101}, C_{1465}) enclosed entirely (100%) with {100} surfaces. The set of fullerenes comprised 7 molecules (C_{60}, C_{180}, C_{320}, C_{540}, C_{720}, C_{960}, C_{1500}), each of them belonging to the I_h point symmetry group. In this study, fullerenes serve as an example of carbon nanoparticles with sp^2-hybridized bonds in contrast to sp^3-bonded nanodiamonds. To complete the picture, we also examined the structure and mechanical properties of nanodiamonds with the hydrogenated surface ($C_{268}H_{144}$, $C_{455}H_{196}$, $C_{660}H_{320}$, and $C_{712}H_{352}$).

All the structures were relaxed using DFT, as described in Sec.2.2. In the case of fullerenes, no dramatic changes in the atomic structure were observed after relaxation. The typical structure with 12 pentagons and I_h-symmetry was preserved. Little changes also occurred in hydrogenated nanodiamonds. Passivation of the surface by hydrogen atoms prevents it from the reconstruction and allows the bulk diamond structure to be preserved almost unchanged. Only small fluctuations in bond lengths and angles were observed in the relaxed structures. Therefore, they could be regarded as slightly distorted fragments of diamond crystal and should have mechanical properties similar to that of a crystalline diamond.

On the contrary, significant structural changes take place in bare nanodiamonds during relaxation. The presence of dangling bonds leads to the rearrangement of atoms on a surface, and peculiarities of this surface reconstruction strongly depend on surface morphology. Despite the presence of {111} surfaces in cuboctahedral nanodiamonds, their proportion is not very large, and {100}

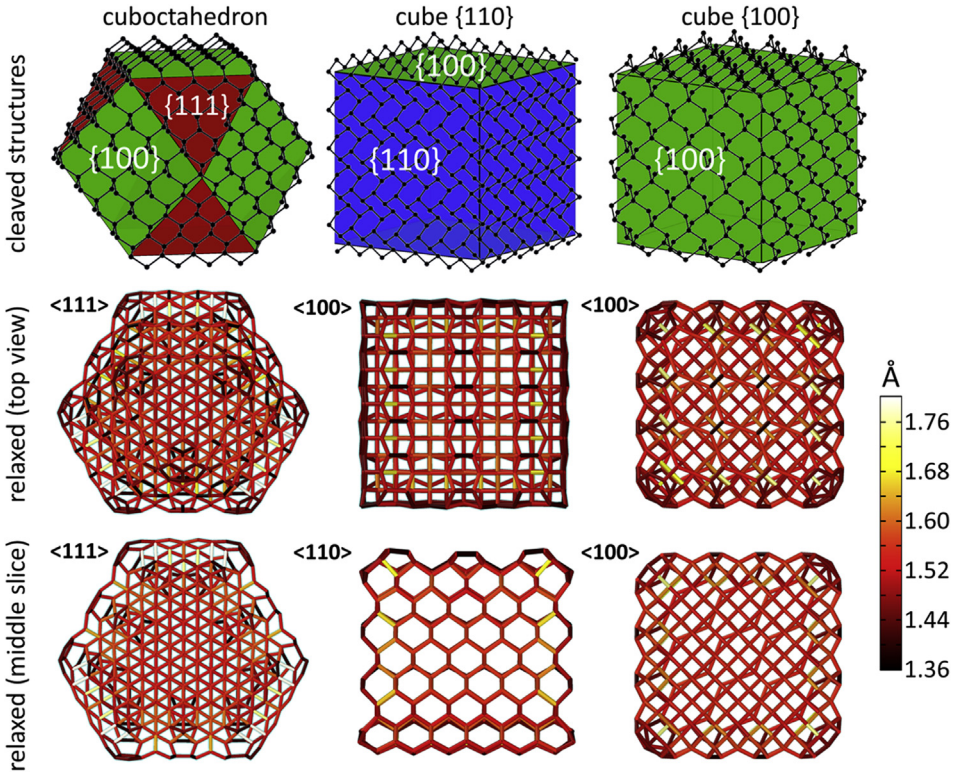

Fig. 2. Zoo of studied nanodiamonds. Top row: Examples of cleaved atomic structures of nanodiamonds superposed onto the sketches of considered geometrical shapes (left to right): cuboctahedral and two families of cubic clusters with different faceting. For clarity, only surficial atoms are shown in the structures. Middle and bottom row: Relaxed atomic structures and color map of bond length distribution (top view and middle slice, respectively). View directions are indicated in the picture. This figure was created using OVITO [51] software. (A colour version of this figure can be viewed online.)

faces are predominant. This prevents cuboctahedral nanodiamonds from delamination of {111} planes, although bonds in this region elongate to 1.60 – 1.75 Å. Reconstruction of {100} surfaces in nanodiamonds occurs similar to the reconstruction of (100) surface in the bulk [52], primarily resulting in the formation of 2 × 1 dimer rows on the faces. In nanodiamonds from cuboctahedral and cube {100} subsets, characteristic fullerene-like caps [53] are present in the corners. These caps are composed of well-pronounced pentagons with the bond lengths (1.42 – 1.46 Å) and angles (~106° – 109°) that are almost identical to values observed in fullerenes (1.45 Å, 108°). The least structural changes were observed in nanodiamonds from cube {110} subset, where only moderate lattice distortions on {110} surfaces (in consistence with {110} bulk diamond surface reconstruction [54]) accompanied with the aforementioned formation of 2 × 1 dimers on {100} faces were found. The examples of relaxed nanodiamonds structures are shown in Fig. 2. More details about the structural properties of nanodiamonds could be also found in the literature [55,56].

Generally speaking, the surface reconstruction that occurs in nanodiamonds results in the substantial transformations of the original sp^3-bonds of diamond. Some bonds in bare nanodiamonds turn into sp^2-like ones, whereas others remain closer to sp^3-bonds but in the strained state. However, there is a common trend towards a predominant presence of shortened (in comparison with the bulk) bonds over the lengthened ones, although the degree of predominance depends on the nanodiamonds' morphology. This trend could be clearly seen from color maps of bond length distribution in nanodiamonds given in Fig. 2. We believe that the effect of bonds shortening in nanodiamonds has a key influence on their mechanical properties, to the discussion of which we turn.

3.3. Mechanical stiffness

To calculate nanostructures' mechanical stiffness, their relaxed atomic structures were subjected to small uniform isotropic deformations (were slightly expanded or compressed) with the following constrained geometry optimization to evaluate their total energy. The constraints are mandatory when performing simulations of the strained nanostructures because otherwise, they would simply go back to the relaxed state due to the absence of periodic boundary conditions on their surface. We found that it is enough to freeze only surficial carbon atoms that have fewer than 4 neighbors to keep structures in the stressed state, whereas all other atoms can be allowed to relax during optimization.

To be able to evaluate bulk modulus of the structure, one should determine its volume. However, there are various ways to determine volume on the atomic scale. In this study, we compared two main approaches to the calculation of nanostructures volume. In the first one, the structure is considered as a continuum medium bounded by an outer shell that has no thickness. The size of atoms is neglected, and nanostructure volume is calculated as volume enclosed by the convex hull of all atoms. For fullerenes, this coincides with the volume used by Ruoff et al. [20,21]. In the following text, we recall this definition as a solid medium volume (V^{solid}).

The second main approach implies the finite size of atoms which can be taken into account in different ways. For nanodiamonds, we evaluated van der Waals volume (V^{vdW}). Atoms were imagined as spheres which can intersect and overlap, and V^{vdW} was found as a total volume of these spheres. To compute V^{vdW} we used the freeware ASV by Petitjean [57] and set the radius of carbon atoms to be equal $r_C = 1.7$ Å following the work of Bondi [58]. For

fullerenes, we calculated an elastic shell volume (V^{shell}) as a volume of a hollow sphere with the thickness t of its shell. This definition is very convenient for hollow nanostructures and allows for direct comparison by mechanical properties with graphene sheet (which is an infinite limit of fullerenes) having the same thickness t. As there is a wide scatter of wall thickness values for CNTs (0.66–3.4 Å), we find it possible to vary fullerenes shell thickness in the same range, as these carbon nanostructures are closely related. For briefness, we present results only for $t = 3.4$ Å in the main body of the article with others available in Supplementary Materials.

Calculations of bulk modulus were carried out for solid medium (B_0^{solid}), van der Waals (B_0^{vdW}) and elastic shell (B_0^{shell}) volume definitions using the unified methodology. The obtained energy vs. volume curves were approximated by the Birch-Murnaghan EOS [59,60] to retrieve B_0. Calculations with linear strains of $\varepsilon = \pm 0.015, \pm 0.03$ were performed in all cases as we found 5 points in the dataset (including relaxed structure) to be enough to gain accurate results. The acquired results are shown in Fig. 3a. A significant stiffening of nanodiamonds in comparison with crystalline diamond is observed. This effect is present in both approaches to volume calculation and can be explained by the predominant presence of shortened (and therefore stiffened) bonds in the structures (Fig. 2). Moreover, we found that the dependence of bulk modulus on nanostructures size has a hyperbolic character that also reflects the contribution of surficial atoms. This size dependence could be fitted by one hyperbola for all nanodiamonds families, that speaks of no significant influence of nanodiamonds shape on their mechanical stiffness.

Nevertheless, different volume definitions lead to discrepant bulk moduli, and in all cases B_0^{vdW} values are higher than the values of B_0^{solid}. Indeed, volumetric deformations corresponding to V^{vdW} are significantly lower than the deformations computed in terms of V^{solid} that results in the steeper $E(\delta)$ curves (see Fig. S1a in Supplementary Materials) and, as a consequence, leads to an increase of the calculated B_0. Moreover, for fullerenes regarded volume definitions lead to completely different trends. On the one hand, B_0^{shell} tends to the constant value close to the effective bulk modulus of graphene (we defined this quantity as $B_0^{eff} = \frac{\gamma_0}{t} \approx 611$ GPa for $t = 3.4$ Å). On the other hand, monotonous fall via hyperbolic law is observed for B_0^{solid} due to a significant volume of a void inside fullerene, which is not included in V^{shell}.

Thus, different approaches to the computation of volume result in different values of bulk modulus, and it is not clear in advance which values of B_0 one should use to characterize the rigidity of the structure. To overcome this problem, we propose an alternative approach of average bond stiffness k_0. This physical quantity has an important advantage in comparison with bulk modulus, as it does not require to estimate structures volume. This relieves from uncertainties which we discussed above and makes the value of k_0 unambiguous.

To calculate k_0, we built bond lengths distribution at each step of deformation for all the structures to find the total number of bonds N_b and their average length l, and then Eq. (1) was used to retrieve k_0. The obtained results are represented in Fig. 3b. As it follows from the figure, values of k_0 are scattered in the range between diamond and graphene bond stiffnesses. Let us point out that all studied nanodiamonds with bare surface overwhelm bulk diamond by the average bond stiffness that increases with decreasing their size, whereas k_0 of hydrogenated nanodiamonds is lower than in crystal and does not manifest any size dependence. This is one more evidence showing that the nanodiamonds stiffness is completely determined by the properties of constituting chemical bonds. As for fullerenes, with their enlargement average bond stiffness tends to the constant value corresponding to graphene (Table 1). Thus, k_0 correctly reproduces the main trends and limiting cases of the considered nanostructures stiffness.

The obtained results can be compared to experimental and theoretical data (Table 2). As one can see, experimentally measured values of nanodiamonds bulk modulus fall in the range predicted by our *ab initio* calculations. As there are no available experimental data on the compressibility of single fullerene molecules (at least, to our knowledge), we compare our results for C_{60} with the previous theoretical works. Again, a good coherence in numbers is observed for both B_0 and k_0 with the results of Ruoff et al. [21] and Peón-Escalante et al. [22].

To gain a deeper insight into the nature of average bond stiffness as a mechanical characteristic of a nanostructure, we expressed it as a weighted sum over all bonds stiffness constants: $k_0^{est} = \frac{\sum k_i}{N_b}$. The validity of this approach is justified by the localized character of covalent bonding in carbon materials (except for graphite and onions, where van der Waals bonding between the layers is present), that allows representing the total energy as a sum of energies per bond $E = \sum E_i$ and associating individual stiffness constant with each bond. The similar concept of atomic bulk modulus was successfully exploited by Kleovoulou et al. [61,62] in studies of silicon nanocrystals local rigidity and in our previous paper about polymerized fullerenes stiffness [6].

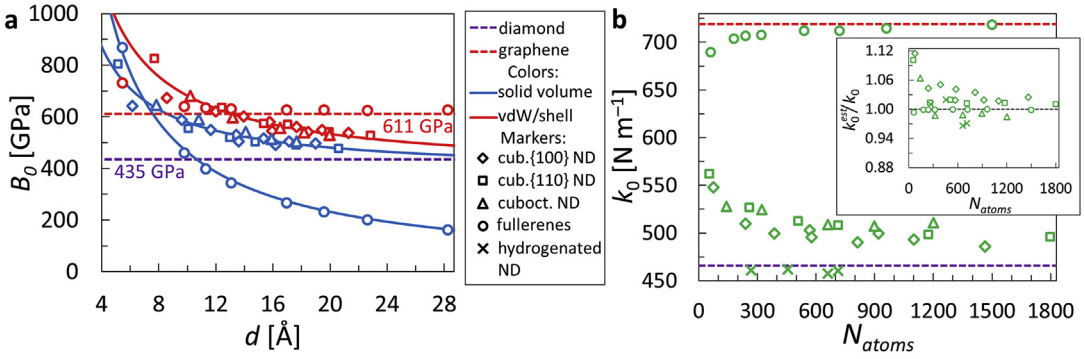

Fig. 3. (a) Size dependence of considered nanostructures B_0 for different volume definitions which are shown in different colors (see the legend). Bulk moduli were retrieved from Birch-Murnaghan approximation of energy-volume curves. Various families of studied nanostructures are displayed with different markers. Hyperbolic fitting for each volume definition is also shown with a solid line of the corresponding color. The size d of nanostructures was determined as a cubic root of the corresponding volume. (b) Average bond stiffness k_0 vs. the number of atoms in nanostructures N_{atoms}. Purple and red dashed lines are given for reference and mark bond stiffness in bulk diamond and graphene, respectively. Ratio of k_0^{est} calculated based on bond lengths distribution to directly calculated stiffness k_0 is drawn in the inset. The black dashed line denotes unity and is drawn to guide an eye. The legend in the figure applies both to frames (a) and (b). (A colour version of this figure can be viewed online.)

Table 2
Values of B_0 and k_0 for nanodiamonds and C_{60} fullerene.

	Nanodiamonds		Fullerene C_{60}	
	present work	experiment	present work	previous theory
Bulk modulus B_0 [GPa]	480 – 670	564[a], 607[b]	868	826[c], 874[d]
Average bond stiffness k_0 [N m^{-1}]	485 – 562	–	689.9	672[c], 691[d]

[a] Ref. [14].
[b] Ref. [15].
[c] Ref. [21].
[d] Ref. [22].

Relying on the number of neighbors, values of bond length and bond angles, we assigned the most appropriate by these structural parameters type of hybridization (sp^2 or sp^3) to each bond (technical details are presented in Supplementary Materials). Further, we used the dependence of bond stiffness on bond length for sp^2-and sp^3-hybridized carbon (Fig. 1b) to calculate k_i and then k_0^{est}. Acquired results (see the inset in Fig. 3b) demonstrate good agreement between k_0^{est} and k_0 with most errors less than 5% which is decreasing with nanostructures enlargement. The fact that directly calculated k_0 can be decomposed on a sum of individual bond stiffness constants directly indicates that the effect of nanodiamonds stiffening could be entirely explained and understood from the consideration of chemical bonds in the studied structures. This fact also confirms that the freezing of the surface atoms seems not to influence strongly the obtained values of k_0, since k_0^{est} is not affected by any constraints and nevertheless, shows good agreement with k_0. Moreover, the mentioned procedure gives an opportunity to estimate the value of the average bond stiffness having only relaxed atomic geometry of the structure. In principle, this relieves from the need for optimizations of strained structure geometry (with frozen surficial atoms) or may be used to verify the results of such direct calculations. We suppose this to be an appealing advantage of our approach from the computational point of view.

Thus, k_0 is a convenient and reliable quantity characterizing the mechanical properties of nanostructures locally. To find the relation between k_0 and B_0 (which should describe stiffness of the structure as a whole), Eq. (3) should be used. It enables to recalculate average bond stiffness into bulk modulus for a given relationship $\delta(\varepsilon)$ under hydrostatic compression conditions, which depends on the chosen definition of volume. For the volumes considered here, we have (see the derivation in Supplementary Materials):

$$B_0^{est} = k_0 \cdot \frac{N_b l_0^2}{9V_0^{solid}}, \tag{5}$$

$$B_0^{est} = k_0 \cdot \frac{N_b l_0^2}{9V_0^{vdW}} \cdot \left(1 + \frac{2r_C}{a_0}\right)^2, \tag{6}$$

$$B_0^{est} = k_0 \cdot \frac{N_b l_0^2}{4V_0^{shell}}. \tag{7}$$

The results in Fig. 4 show that the suggested method allows estimating nanostructures bulk modulus with an accuracy of 14% at worst and works much better in most cases. The error reduces with increasing nanostructures size, and thus reasonable estimates of B_0 can be obtained using Eqs. (5) – (7). These equations are approximate, but in principle, the exact ones can be obtained using the same ideas. However, we suppose that this is not required for the purposes of a rough estimate, especially since bulk modulus is ambiguous on the nanoscale by its nature. We believe that the obtained results provide both qualitative as well as a quantitative understanding of the intrinsic relationship between bulk modulus and average bond stiffness. We also found that after a small modification the proposed method is capable of describing mechanical properties of defective structures (see Supplementary Materials).

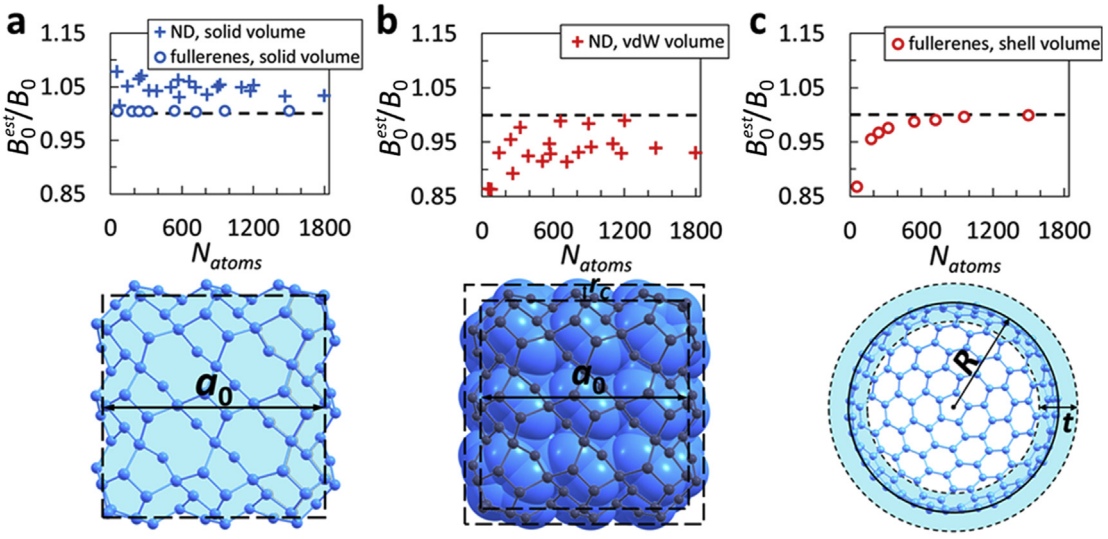

Fig. 4. Ratio of B_0^{est} to directly calculated bulk modulus B_0 for different volume definitions: (a) solid medium volume, (b) van der Waals volume, (c) elastic shell volume. Illustrations to the considered volume definitions are represented in the bottom. (A colour version of this figure can be viewed online.)

However, the average bond stiffness approach also has its own limitations. By its definition postulating that strain energy is more or less uniformly distributed by individual chemical bonds in the structure, the usage of k_0 for characterizing nanostructure stiffness is restricted to the case of covalently bonded solids. For instance, k_0 cannot be applied for the description of layered nanostructures where van der Waals interactions play an important role (*e.g.*, carbon onions and onion-like structures). Indeed, the application of moderate external pressure to such structures should lead only to outer shell compression whereas inner core would remain almost undistorted. Therefore, the average bond stiffness approach would give much higher stiffness values that do not make any physical sense in such cases (see Supplementary Materials for additional discussion).

4. Conclusions

Based on our findings, we conclude that average bond stiffness should be considered as a primary characteristic of mechanical stiffness on the nanoscale. k_0 enables one to unambiguously determine which structure is stiffer whether it is a bulk crystal or low-dimensional object. This could be done basing only on relaxed atomic geometry that is the important advantage of this method. In principle, this approach could be applied to studies of any carbon nanostructures (*e.g.*, nanorods, nanoribbons), provided that they are covalently bound. Moreover, there are no restrictions for extending this method to nanostructures composed by other elements capable of forming covalent solids, such as Si, Ge *etc*. Thus, there is a wide scope for further investigations, and we believe that our results could be useful for future works in this area.

Authors contributions

Almaz Khabibrakhmanov: Methodology, Software, Investigation, Writing – Original Draft.

Pavel Sorokin: Conceptualization, Writing – Review & Editing, Supervision.

Declaration of competing interest

The authors declare that they have no known competing financial interests or personal relationships that could have appeared to influence the work reported in this paper.

Acknowledgments

This work was funded by the Russian Foundation for Basic Research grant #18-29-19019. We also acknowledge the financial support of the Ministry of Education and Science of the Russian Federation in the framework of Increase Competitiveness Program of NUST “MISiS” (No. K2-2019-016) and Grant of President of Russian Federation for government support of young DSc. (MD-1046.2019.2). The calculations were performed at the supercomputer cluster provided by the Materials Modeling and Development Laboratory at NUST “MISiS”. We are grateful to Prof. David Tománek for the fruitful discussion.

Appendix A. Supplementary data

Supplementary data to this article can be found online at https://doi.org/10.1016/j.carbon.2019.12.071.

References

[1] J.J. Gilman, Why diamond is very hard, Philos. Mag. A 82 (2002) 1811–1820, https://doi.org/10.1080/01418610208235692.
[2] M.M.J. Treacy, T.W. Ebbesen, J.M. Gibson, Exceptionally high Young’s modulus observed for individual carbon nanotubes, Nature 381 (1996) 678–680, https://doi.org/10.1038/381678a0.
[3] E.W. Wong, P.E. Sheehan, C.M. Lieber, Nanobeam mechanics: elasticity, strength, and toughness of nanorods and nanotubes, Science 277 (1997), https://doi.org/10.1126/science.277.5334.1971, 1971–1975.
[4] A. Krishnan, E. Dujardin, T.W. Ebbesen, P.N. Yianilos, M.M.J. Treacy, Young’s modulus of single-walled nanotubes, Phys. Rev. B. 58 (1998) 14013–14019, https://doi.org/10.1103/PhysRevB.58.14013.
[5] V.D. Blank, S.G. Buga, G.A. Dubitsky, N.R. Serebryanaya, M.Y. Popov, B. Sundqvist, High-pressure polymerized phases of C60, Carbon 36 (1998) 319–343, https://doi.org/10.1016/S0008-6223(97)00234-0.
[6] Y.A. Kvashnina, A.G. Kvashnin, M.Y. Popov, B.A. Kulnitskiy, I.A. Perezhogin, E.V. Tyukalova, L.A. Chernozatonskii, P.B. Sorokin, V.D. Blank, Toward the ultra-incompressible carbon materials. Computational simulation and experimental observation, J. Phys. Chem. Lett. 6 (2015) 2147–2152, https://doi.org/10.1021/acs.jpclett.5b00748.
[7] Y.A. Kvashnina, A.G. Kvashnin, L.A. Chernozatonskii, P.B. Sorokin, Fullerite-based nanocomposites with ultrahigh stiffness, Theor. Invest. Carbon 115 (2017) 546–549, https://doi.org/10.1016/j.carbon.2017.01.028.
[8] C. Lee, X. Wei, J.W. Kysar, J. Hone, Measurement of the elastic properties and intrinsic strength of monolayer graphene, Science 321 (2008) 385–388, https://doi.org/10.1126/science.1157996.
[9] J.-U. Lee, D. Yoon, H. Cheong, Estimation of young’s modulus of graphene by Raman spectroscopy, Nano Lett. 12 (2012) 4444–4448, https://doi.org/10.1021/nl301073q.
[10] O.A. Shenderova, V.V. Zhirnov, D.W. Brenner, Carbon nanostructures, Crit. Rev. Solid State Mater. Sci. 27 (2002) 227–356, https://doi.org/10.1080/10408430208500497.
[11] V.N. Mochalin, O. Shenderova, D. Ho, Y. Gogotsi, The properties and applications of nanodiamonds, Nat. Nanotechnol. 7 (2012) 11–23, https://doi.org/10.1038/nnano.2011.209.
[12] T. Irifune, A. Kurio, S. Sakamoto, T. Inoue, H. Sumiya, Ultrahard polycrystalline diamond from graphite, Nature 421 (2003) 599–600, https://doi.org/10.1038/421599b.
[13] Q. Huang, D. Yu, B. Xu, W. Hu, Y. Ma, Y. Wang, Z. Zhao, B. Wen, J. He, Z. Liu, Y. Tian, Nanotwinned diamond with unprecedented hardness and stability, Nature 510 (2014) 250–253, https://doi.org/10.1038/nature13381.
[14] M. Popov, V. Churkin, A. Kirichenko, V. Denisov, D. Ovsyannikov, B. Kulnitskiy, I. Perezhogin, V. Aksenenkov, V. Blank, Raman spectra and bulk modulus of nanodiamond in a size interval of 2–5 nm, Nanoscale Res. Lett. 12 (2017) 1–6, https://doi.org/10.1186/s11671-017-2333-0.
[15] M. Popov, V. Churkin, D. Ovsyannikov, A. Khabibrakhmanov, A. Kirichenko, E. Skryleva, Y. Parkhomenko, M. Kuznetsov, S. Nosukhin, P. Sorokin, S. Terentiev, V. Blank, Ultrasmall diamond nanoparticles with unusual incompressibility, Diam. Relat. Mater. 96 (2019) 52–57, https://doi.org/10.1016/j.diamond.2019.04.033.
[16] Y. Huang, J. Wu, K.C. Hwang, Thickness of graphene and single-wall carbon nanotubes, Phys. Rev. B. 74 (2006) 245413, https://doi.org/10.1103/PhysRevB.74.245413.
[17] C.Y. Wang, L.C. Zhang, A critical assessment of the elastic properties and effective wall thickness of single-walled carbon nanotubes, Nanotechnology 19 (2008) 75705, https://doi.org/10.1088/0957-4484/19/7/075705.
[18] B.I. Yakobson, C.J. Brabec, J. Bernholc, Nanomechanics of carbon tubes: instabilities beyond linear response, Phys. Rev. Lett. 76 (1996) 2511–2514, https://doi.org/10.1103/PhysRevLett.76.2511.
[19] J. Cai, C.Y. Wang, T. Yu, S. Yu, Wall thickness of single-walled carbon nanotubes and its Young’s modulus, Phys. Scr. 79 (2009) 25702, https://doi.org/10.1088/0031-8949/79/02/025702.
[20] R.S. Ruoff, A.L. Ruoff, Is C60 stiffer than diamond? Nature 350 (1991) 663–664, https://doi.org/10.1038/350663b0.
[21] R.S. Ruoff, A.L. Ruoff, The bulk modulus of C $_{60}$ molecules and crystals: a molecular mechanics approach, Appl. Phys. Lett. 59 (1991) 1553–1555, https://doi.org/10.1063/1.106280.
[22] R. Peón-Escalante, C. Villanueva, R. Quintal, F. Avilés, A. Tapia, The bond force constant and bulk modulus of C60, Comput. Mater. Sci. 83 (2014) 120–126, https://doi.org/10.1016/j.commatsci.2013.11.011.
[23] C. Li, T.-W. Chou, A structural mechanics approach for the analysis of carbon nanotubes, Int. J. Solids Struct. 40 (2003) 2487–2499, https://doi.org/10.1016/S0020-7683(03)00056-8.
[24] R.C. Andrew, R.E. Mapasha, A.M. Ukpong, N. Chetty, Mechanical properties of graphene and boronitrene, Phys. Rev. B 85 (2012) 125428, https://doi.org/10.1103/PhysRevB.85.125428.
[25] P. Hohenberg, W. Kohn, Inhomogeneous electron gas, Phys. Rev. 136 (1964) B864–B871, https://doi.org/10.1103/PhysRev.136.B864.
[26] W. Kohn, L.J. Sham, Self-consistent equations including exchange and correlation effects, Phys. Rev. 140 (1965) A1133–A1138, https://doi.org/10.1103/PhysRev.140.A1133.
[27] P.E. Blöchl, Projector augmented-wave method, Phys. Rev. B 50 (1994) 17953–17979, https://doi.org/10.1103/PhysRevB.50.17953.
[28] G. Kresse, D. Joubert, From ultrasoft pseudopotentials to the projector augmented-wave method, Phys. Rev. B 59 (1999) 1758–1775, https://doi.org/10.1103/PhysRevB.59.1758.
[29] G. Kresse, J. Furthmüller, Efficient iterative schemes for *ab initio* total-energy

calculations using a plane-wave basis set, Phys. Rev. B 54 (1996) 11169–11186, https://doi.org/10.1103/PhysRevB.54.11169.
[30] G. Kresse, J. Furthmüller, Efficiency of ab-initio total energy calculations for metals and semiconductors using a plane-wave basis set, Comput. Mater. Sci. 6 (1996) 15–50, https://doi.org/10.1016/0927-0256(96)00008-0.
[31] J.P. Perdew, K. Burke, M. Ernzerhof, Generalized gradient approximation made simple, Phys. Rev. Lett. 77 (1996) 3865–3868, https://doi.org/10.1103/PhysRevLett.77.3865.
[32] H.J. Monkhorst, J.D. Pack, Special points for Brillouin-zone integrations, Phys. Rev. B 13 (1976) 5188–5192, https://doi.org/10.1103/PhysRevB.13.5188.
[33] F. Occelli, P. Loubeyre, R. LeToullec, Properties of diamond under hydrostatic pressures up to 140 GPa, Nat. Mater. 2 (2003) 151–154, https://doi.org/10.1038/nmat831.
[34] D.K. Bradley, J.H. Eggert, R.F. Smith, S.T. Prisbrey, D.G. Hicks, D.G. Braun, J. Biener, A.V. Hamza, R.E. Rudd, G.W. Collins, Diamond at 800 GPa, Phys. Rev. Lett. 102 (2009) 75503, https://doi.org/10.1103/PhysRevLett.102.075503.
[35] P. Vinet, J.R. Smith, J. Ferrante, J.H. Rose, Temperature effects on the universal equation of state of solids, Phys. Rev. B. 35 (1987) 1945–1953, https://doi.org/10.1103/PhysRevB.35.1945.
[36] F. Birch, Finite strain isotherm and velocities for single-crystal and polycrystalline NaCl at high pressures and 300°K, J. Geophys. Res. 83 (1978) 1257–1268, https://doi.org/10.1029/JB083iB03p01257.
[37] J. Xie, S.P. Chen, J.S. Tse, S. de Gironcoli, S. Baroni, High-pressure thermal expansion, bulk modulus, and phonon structure of diamond, Phys. Rev. B 60 (1999) 9444–9449, https://doi.org/10.1103/PhysRevB.60.9444.
[38] F. Zhi-Jian, J. Guang-Fu, C. Xiang-Rong, G. Qing-Quan, First-principle calculations for elastic and thermodynamic properties of diamond, Commun. Theor. Phys. 51 (2009) 1129–1134, https://doi.org/10.1088/0253-6102/51/6/31.
[39] X. Wei, B. Fragneaud, C.A. Marianetti, J.W. Kysar, Nonlinear elastic behavior of graphene: *Ab initio* calculations to continuum description, Phys. Rev. B. 80 (2009) 205407, https://doi.org/10.1103/PhysRevB.80.205407.
[40] Y. Baskin, L. Meyer, Lattice constants of graphite at low temperatures, Phys. Rev. 100 (1955) 544, https://doi.org/10.1103/PhysRev.100.544.
[41] A. Bosak, M. Krisch, M. Mohr, J. Maultzsch, C. Thomsen, Elasticity of single-crystalline graphite: inelastic x-ray scattering study, Phys. Rev. B. 75 (2007) 153408, https://doi.org/10.1103/PhysRevB.75.153408.
[42] Y.X. Zhao, I.L. Spain, X-ray diffraction data for graphite to 20 GPa, Phys. Rev. B. 40 (1989) 993–997, https://doi.org/10.1103/PhysRevB.40.993.
[43] K. Kunc, I. Loa, K. Syassen, Equation of state and phonon frequency calculations of diamond at high pressures, Phys. Rev. B. 68 (2003) 94107, https://doi.org/10.1103/PhysRevB.68.094107.
[44] J. Paier, M. Marsman, K. Hummer, G. Kresse, I.C. Gerber, J.G. Ángyán, Screened hybrid density functionals applied to solids, J. Chem. Phys. 124 (2006) 154709, https://doi.org/10.1063/1.2187006.
[45] Y.S. Touloukian, R.K. Kirby, R.E. Taylor, T.Y.R. Lee, Thermal Expansion, Springer US, Boston, MA, 1977.
[46] A. Dewaele, F. Datchi, P. Loubeyre, M. Mezouar, High pressure–high temperature equations of state of neon and diamond, Phys. Rev. B. 77 (2008) 94106, https://doi.org/10.1103/PhysRevB.77.094106.
[47] M. Hanfland, H. Beister, K. Syassen, Graphite under pressure: equation of state and first-order Raman modes, Phys. Rev. B. 39 (1989) 12598–12603, https://doi.org/10.1103/PhysRevB.39.12598.
[48] O.L. Blakslee, D.G. Proctor, E.J. Seldin, G.B. Spence, T. Weng, Elastic constants of compression-annealed pyrolytic graphite, J. Appl. Phys. 41 (1970) 3373–3382, https://doi.org/10.1063/1.1659428.
[49] H.J. McSkimin, W.L. Bond, Elastic moduli of diamond, Phys. Rev. 105 (1957) 116–121, https://doi.org/10.1103/PhysRev.105.116.
[50] R. Vogelgesang, A.K. Ramdas, S. Rodriguez, M. Grimsditch, T.R. Anthony, Brillouin and Raman scattering in natural and isotopically controlled diamond, Phys. Rev. B. 54 (1996) 3989–3999, https://doi.org/10.1103/PhysRevB.54.3989.
[51] A. Stukowski, Visualization and analysis of atomistic simulation data with OVITO–the Open Visualization Tool, Model. Simul. Mater. Sci. Eng. 18 (2010) 15012, https://doi.org/10.1088/0965-0393/18/1/015012.
[52] J. Furthmüller, J. Hafner, G. Kresse, Dimer reconstruction and electronic surface states on clean and hydrogenated diamond (100) surfaces, Phys. Rev. B. 53 (1996) 7334–7351, https://doi.org/10.1103/PhysRevB.53.7334.
[53] J.-Y. Raty, G. Galli, C. Bostedt, T. van Buuren, L. Terminello, Quantum confinement and fullerenelike surface reconstructions in nanodiamonds, Phys. Rev. Lett. 90 (2003) 37401, https://doi.org/10.1103/PhysRevLett.90.037401.
[54] G. Kern, J. Hafner, *Ab initio* calculations of the atomic and electronic structure of clean and hydrogenated diamond (110) surfaces, Phys. Rev. B. 56 (1997) 4203–4210, https://doi.org/10.1103/PhysRevB.56.4203.
[55] A.S. Barnard, S.P. Russo, I.K. Snook, Structural relaxation and relative stability of nanodiamond morphologies, Diam. Relat. Mater. 12 (2003) 1867–1872, https://doi.org/10.1016/S0925-9635(03)00275-9.
[56] A.S. Barnard, M. Sternberg, Crystallinity and surface electrostatics of diamond nanocrystals, J. Mater. Chem. 17 (2007) 4811–4819, https://doi.org/10.1039/b710189a.
[57] M. Petitjean, On the analytical calculation of van der Waals surfaces and volumes: some numerical aspects, J. Comput. Chem. 15 (1994) 507–523, https://doi.org/10.1002/jcc.540150504.
[58] A. Bondi, van der Waals volumes and radii, J. Phys. Chem. 68 (1964) 441–451, https://doi.org/10.1021/j100785a001.
[59] F.D. Murnaghan, The compressibility of media under extreme pressures, Proc. Natl. Acad. Sci. 30 (1944) 244–247, https://doi.org/10.1073/pnas.30.9.244.
[60] F. Birch, Finite elastic strain of cubic crystals, Phys. Rev. 71 (1947) 809–824, https://doi.org/10.1103/PhysRev.71.809.
[61] K. Kleovoulou, P.C. Kelires, Stress state of embedded Si nanocrystals, Phys. Rev. B. 88 (2013) 85424, https://doi.org/10.1103/PhysRevB.88.085424.
[62] K. Kleovoulou, P.C. Kelires, Local rigidity and physical trends in embedded Si nanocrystals, Phys. Rev. B. 88 (2013) 245202, https://doi.org/10.1103/PhysRevB.88.245202.